Multislit interferometry and commuting functions of position and momentum

Johannes C. G. Biniok* and Paul Busch†
University of York, York YO10 5DD, United Kingdom
(Received 26 April 2013; published 21 June 2013)

In a recent, modified double-pinhole diffraction experiment the existence of an interference pattern was established indirectly along with a near-perfect imaging of the double pinhole. Our theoretical analysis shows that the experiment constitutes a preparation of a quantum state that is, to a good approximation, a joint eigenstate of commuting functions of position and momentum. Gaining information about the momentum distribution by means of the particular experimental setup is thus possible with negligible impact on the position distribution. Furthermore, we construct explicitly a class of states simultaneously localized on periodic sets in position and momentum space, which are therefore eigenstates of the observables being measured jointly (to a good approximation) in multislit interferometry. Finally, we show that with an appropriate change of settings the experiment demonstrates the mutual disturbance of position and momentum measurements.

DOI: 10.1103/PhysRevA.87.062116 PACS number(s): 03.65.−w

I. INTRODUCTION

Still at the heart of quantum mechanics, the double-slit experiment remains the subject of ongoing investigation with surprising results that attract wide attention. For example, a recent interference experiment [1] exhibited "average trajectories" via weak measurements. Here, we revisit another experiment, reported in 2007 [2], which investigates the influence of a wire grating placed at the nodes of the interference pattern on the image of the double pinhole. While the authors' own theoretical account has been criticized, the experiment itself remains interesting. As we argue here, in this experiment a quantum state is prepared that is approximately a joint eigenstate of position and momentum on periodic sets, and verified with negligible disturbance.

Multislit interference experiments, such as Young's double-slit experiment, consist of a coherent source, an aperture mask, and a detection screen (placed in the far field). Within the framework of quantum mechanics, such an experiment is viewed as follows: While the aperture mask prepares a particle in a quantum state with a certain position distribution, the observed interference pattern is a measurement of the associated momentum distribution.

Traditionally, the momentum distribution is captured on a detection screen, but this clearly destroys the quantum state. Establishing the existence of an interference pattern indirectly, i.e., without destroying the quantum state, is possible by removing the screen and replacing it by a wire grating, each wire carefully placed at the location of a node in the interference pattern [2]. The existence of an interference pattern may be deduced from the practically undiminished intensity passing the wire grating. Using a lens, a geometric image of the aperture is produced, which allows detection of the quantum particle on the very set of positions it was prepared on—after it was subjected to a momentum measurement. While indirectly observing an interference pattern without changing the localization properties of a system may not be surprising from the point of view of classical physics, it is rather curious when considered in terms of quantum mechanics: Information about a quantum state was obtained, but apparently without changing the properties of that quantum state. In particular, information about a pair of incompatible observables was obtained; in this context, the measurement seems "classical," revealing already existing information without changing the system properties.

This observation indicates that the experiment should be described in terms of two commuting observables which yield information about position and momentum, respectively. While position and momentum do not commute, functions of position may commute with functions of momentum. Indeed, as will be shown here, the experiment can be considered an approximate realization of a joint eigenstate of mutually commuting functions of position and momentum. In the next two sections, the experimental setup and joint eigenstates of periodic sets of position and momentum are discussed. This is followed by a description of multislit experiments in terms of joint eigenstates.

The experiment reported in [2] was performed with photons; its analysis would require a treatment in terms of photons as massless spin-1 particles, which are known to be only unsharply localizable. (A review of the problem of photon localization and relevant literature where unsharp localization observables for the photon are introduced can be found in [3].) For simplicity, the treatment here is nonrelativistic and strictly only applies to matter waves. There is nevertheless good qualitative and quantitative agreement between our theoretical analysis and the experiment, suggesting that an analog of the nonrelativistic argument applicable to photons should exist, and showing that the experiment demonstrates a simultaneous determination of compatible, coarse-grained versions of the complementary position and momentum observables.

II. ON THE EXPERIMENTAL SETUP

The setup illustrated in Fig. 1 depicts a simplified version of the experiment reported in [2]. While the experiment was performed using a double pinhole, here a double-slit setup is considered. A particle propagates through the device along the z axis (from left to right). We model its wave function as a product, $\Psi(x,y,z) = \phi(x)\eta(y)\zeta(z)$, and focus on the

*jcgb500@york.ac.uk
†paul.busch@york.ac.uk

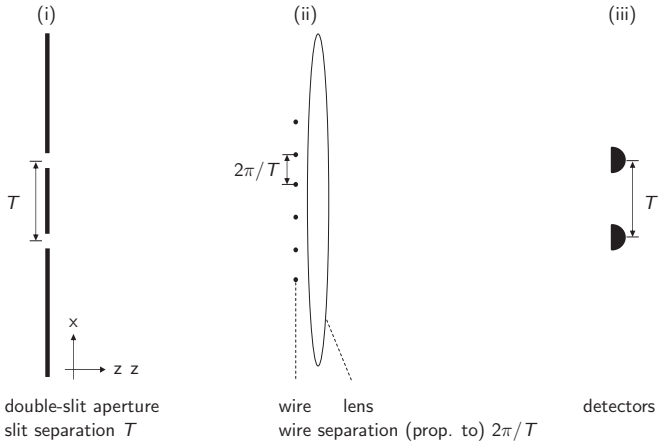

FIG. 1. Simplified illustration of the setup used to indirectly establish the existence of an interference pattern of a coherently illuminated double-slit aperture.

component $\phi(x)$, where the x axis is along the transversal (vertical) direction. The state $\zeta(z)$ is a means of keeping track of the times of passage through the experimental setup. As is detailed in Appendix A and used later on, in the appropriate limit this problem can be simplified so that only $\phi(x)$ needs to be considered, removing any explicit time dependence but retaining an identification of the quantum state at different times with distinct locations in the setup.

The wave function $\phi(x)$ is diffracted at location (i), where the double-slit aperture mask is depicted. A wire grating is placed at location (ii), where the interference pattern would be expected. The separation of the wires depends on the spacing of the slits in the aperture mask via the indicated reciprocal correspondence $T \leftrightarrow 2\pi/T$, although in general the wavelength of the source must be taken into account. A lens is placed immediately behind the wire grating for the purpose of producing the geometrical image of the original aperture at location (iii), where the detectors are placed. As is argued below, the sequential character of the setup, with the aperture at (i) and the grating at (ii), actually constitutes a joint preparation and measurement.

The action of the aperture mask at (i) is modeled by the following transmission function that gives the wave function ψ (up to normalization) after passage through the aperture:

$$\phi(x) \to \chi_A(x)\,\phi(x) \equiv C\psi(x). \tag{1}$$

Here C is a normalization constant and $\chi_A(x)$ is the indicator function of set A, with value 1 for $x \in A$ and 0 otherwise, A being the set that describes the effective aperture. Incidentally, Eq. (1) defines the action of an operator that is defined as a function $\chi_A(Q)$ of the position operator Q:

$$[\chi_A(Q)\,\phi]\,(x) := \chi_A(x)\phi(x).$$

This operator has eigenvalues 1 and 0 with associated eigenfunctions given by functions $\phi(x)$ either localized within A or within the complement of A. Thus, the state vector ϕ is projected onto an eigenvector of the *spectral projector* $\chi_A(Q)$ of Q associated with the set A. For coherent illumination of both slits, a wave function with two isolated peaks is prepared. Such a superposition state is henceforth denoted ψ_2. A single-slit wave function, denoted ψ_1, is used to describe a single-slit state.

The aperture mask at location (i) prepares the quantum state represented by the wave function ψ, which then propagates freely until it arrives at (ii). In the Fraunhofer limit, upon arriving at (ii) the wave function has evolved so as to have a profile approximately identical (up to scaling) to that of the Fourier transform $\widetilde{\psi}$ of the wave function at (i). For more details, the reader is referred to Appendix A.

The effect of the wire grating is modeled by a transmission function similar to the one specified in (1), but with a set B of intervals complementing the regions occupied by the wire grating:

$$\widetilde{\psi}(k) = (\mathcal{F}\psi)(k) \to \chi_B(k)\,\widetilde{\psi}(k) \equiv [\chi_B(P)\,\widetilde{\psi}](k),$$

where the arrow indicates passage through the wire grating and $\chi_B(P)$ denotes the spectral projector of momentum P associated with the set B and $\mathcal{F}$ denotes the unitary operator effecting the Fourier transform,

$$\widetilde{f}(k) = (\mathcal{F}f)(k) = \frac{1}{\sqrt{2\pi}} \int_{-\infty}^{\infty} f(x)\,e^{ikx}\,dx.$$

In the experimental setup of [2], a total of six wires is used, each with a diameter of 0.127 mm and a separation of 1.3 mm. It should be noted that for a single-slit interference pattern the wire grating would not be in the exact center, but shifted sideways by a small amount. (In the experimental setup reported in [2], the wire grating is shifted by 0.250 mm while the single-slit interference pattern is of the order of tens of millimeters.)

Finally, the action of the lens located at (ii) is modeled as spatial inversion, expressed by mappings $Q \mapsto -Q$ and $P \mapsto -P$, for the position and momentum, respectively. This corresponds to the unitary parity transformation $\mathcal{P}$, which coincides with the square of the Fourier transformation $\mathcal{F}$. As a result, the divergent wave rays emerging, say, from the double pinhole and arriving at the wire grating and lens are inverted so as to be refocused into an image of the original double slit.

III. COMMUTING FUNCTIONS OF POSITION AND MOMENTUM

While the canonical commutation relation $[Q,P] = i$ (we will put $\hbar = 1$ throughout) represents the fact that the position and momentum observables are incompatible in a strong sense, a function of position may commute with a function of momentum. A first characterization of commuting functions of position and momentum was given in [4] in the context of an analysis of interference experiments, with the aim of explaining nonlocal momentum transfers in the Aharonov-Bohm effect. A first full proof of necessary and sufficient conditions for the commutativity of functions of position and momentum was was reported in [5], who were unaware of the work of [4]. A first construction of a set of joint eigenstates was given in [6]. Here, we present a construction of joint eigenstates that is readily identified with multislit interferometry. In Appendix C an alternative, rigorous construction is included that generalizes [6].

Considering the commutation relation in a form due to Weyl,

$$e^{ipQ}e^{iqP} = e^{-ipq}e^{iqP}e^{ipQ},$$

the existence of commuting functions of Q and P is suggested since the operators e^{ipQ} and e^{iqP} commute for $pq = 2\pi n$ with $n \in \mathbb{N}$. Though Q and P do not commute, the spectral projections $\chi_X(Q)$ and $\chi_Y(P)$ for periodic sets X and Y commute if the sets have periods T and $2\pi/(nT)$, respectively, where $n \in \mathbb{N}$:

$$[\chi_X(Q), \chi_Y(P)] = 0.$$

[A set X is called periodic with (positive minimal) period T, if T is the smallest positive number by which X can be shifted such that the shifted set $X + T = X$, or equivalently, if its indicator function is a periodic function with minimal period T.]

Physical systems exhibiting such doubly periodic behavior occur naturally. A well known example is found in solid state physics: The wave function of an electron in a crystal is not only periodically localized in accordance with the periodic potential that is due to a crystal lattice; the wave function is also periodically localized in momentum space (this is encapsulated in the notion of the reciprocal lattice). While solid state physics often deals with systems containing a very large (essentially infinite) number of lattice points, even finite multislit experiments can be regarded as an approximate realization of joint eigenstates of $\chi_X(Q)$ and $\chi_Y(P)$ over periodic sets as is argued below.

The following construction of a class of joint eigenvectors is carried out using the Dirac comb Δ_T, defined as

$$\Delta_T(x) = \sum_{n=-\infty}^{\infty} \delta(x - nT),$$

where δ denotes the delta distribution. This has heuristic value and also makes the identification with multislit experiments more intuitive. We note that under a Fourier transformation the Dirac comb Δ_T with period T becomes a Dirac comb with period $2\pi/T$:

$$\mathcal{F}(\Delta_T)(k) = \frac{1}{T}\,\Delta_{2\pi/T}(k). \tag{2}$$

The sought joint eigenstates of $\chi_X(Q)$ and $\chi_Y(P)$ must have position and momentum representations that are localized in the periodic sets X and Y, respectively. Their construction makes use of the following identity involving functions W and M which will be suitably chosen:

$$\mathcal{F}(W * (\Delta_T\, M))(k) = \left[\widetilde{W}\left(\frac{1}{T}\Delta_{\frac{2\pi}{T}} * \widetilde{M}\right)\right](k). \tag{3}$$

The order of the two operations in (3), convolution ($*$) and multiplication, may be chosen freely, though the result is different in general. Here, both orders appear naturally because of the Fourier transformation present. (A special case of (3) is applied in [7] for the construction of functions invariant under Fourier transformation.)

We now choose W and $\widetilde{M}$ to be square-integrable functions that are localized on (that is, vanish exactly outside) intervals of lengths strictly less than T, resp. $2\pi/T$. [It will be convenient to use the mathematical term *support (of a function)* when speaking of the smallest closed set on which the function is localized.] This ensures that the function ψ defined via (3) is indeed square integrable (see Appendix B):

$$\psi(x) = [W * (\Delta_T\, M)](x), \tag{4}$$

$$\widetilde{\psi}(k) = \left[\widetilde{W}\left(\frac{1}{T}\Delta_{2\pi/T} * \widetilde{M}\right)\right](k). \tag{5}$$

The wave function ψ is now localized on a periodic set X with period T, and its Fourier transform $\widetilde{\psi}$ is localized on a periodic set Y with period $2\pi/T$. These sets are indeed obtained by placing equidistant copies of the supports of W and $\widetilde{M}$, respectively. It follows in line with the result of [5] that ψ is a joint eigenstate of the associated spectral projections of position and momentum. A mathematically rigorous construction of such joint eigenstates without the use of Dirac combs is included in the Appendix B.

The vector ψ thus does not change under the action of these spectral projections $\chi_X(Q)$ and $\chi_Y(P)$. In general, for any wave function ϕ, the projected wave function

$$\chi_Y(P)\chi_X(Q)\phi$$

is a joint eigenstate of the two projectors. In fact, all eigenstates with eigenvalue 1 may be obtained as the projection onto the intersection of the ranges of $\chi_X(Q)$ and $\chi_Y(P)$, which is given by the product $\chi_X(Q)\chi_Y(P) = \chi_Y(P)\chi_X(Q)$. In the analysis below we model the action of the slits and wires as projections in this sense.

IV. MULTISLIT EXPERIMENTS IN TERMS OF JOINT EIGENSTATES OF Q AND P ON PERIODIC SETS

As reported in [2], an initial superposition state ψ_2 propagates through the experimental setup nearly undisturbed. By contrast, there is an effect on the image of the single-slit state ψ_1 detected at (iii): In addition to the expected intensity peak many smaller peaks are found, such that each peak is separated by a distance T from its immediate neighbors. An illustration can be found in [2], Figs. 1(c) and 1(d) therein.

These two observations can be understood in terms of joint eigenstates of Q and P on periodic sets. First, the superposition state ψ_2 remains unchanged to a good approximation, because ψ_2 is already prepared at (i) as a good approximation to a joint eigenstate of periodic characteristic functions of position and momentum with appropriate periodic sets X,Y. This makes ψ_2 an approximation to an eigenstate of the momentum projector associated with the opening left by the wire grating, and hence leaves it virtually undisturbed in the presence of the grating. This can be described symbolically by the approximate equations

$$\psi_2 = \chi_X(Q)\psi_2 \to \chi_B(P)\psi_2 \approx \chi_Y(P)\psi_2 = \psi_2' \approx \psi_2.$$

Here $\psi \approx \phi$ is taken to mean $\|\psi - \phi\| \ll 1$ for (sub)normalized vectors; the arrow denotes passage through the wire grating.

Second, the single-slit state ψ_1 does not remain unchanged, but instead is detected on a set of locations expected of a joint eigenstate defined on a periodic set, as described above. It follows that the wire grating imposes nodes in a manner that

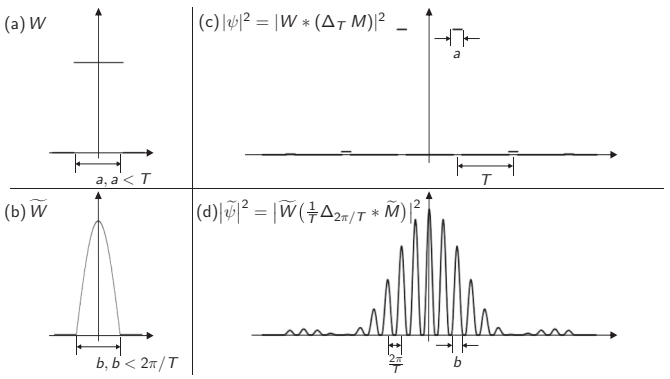

FIG. 2. Illustration of a state localized on periodic sets in position and momentum space. For this particular choice of W, $\widetilde{M}$, the tails of $|\psi|^2$ are negligible outside the two central slits, so that X is well approximated by a double slit, and the negative-outcome testing of the localization of $|\widetilde{\psi}|^2$ within Y does not require many more than ten wires.

approximates the action of $\chi_Y(P)$ to a high degree, because ψ_1 remains an eigenstate of $\chi_X(Q)$ after this action:

$$\psi_1 = \chi_X(Q)\psi_1 \to \chi_Y(P)\psi_1 = \psi_1' = \chi_X(Q)\psi_1' \not\approx \psi_1.$$

Considering that the experimental setup in [2] involves merely six wires, this may seem surprising. Without further analysis of the experimental details, this suggests that the part of the wave function not penetrating the wire grating must have comparatively small amplitude. This is elaborated below.

While all quantum states that pass the aperture mask are eigenstates of $\chi_X(Q)$, the combined effect of aperture and wire grating represents a preparation procedure for approximate joint eigenstates of $\chi_X(Q)$ and $\chi_Y(P)$: All quantum states are projected into the range of $\chi_X(Q)\chi_Y(P) = \chi_Y(P)\chi_X(Q)$ to a good approximation. The superposition state ψ_2 is thus already an approximate eigenstate of both projections, and the effect of the wire grating is much smaller than on the single-slit state ψ_1, and even negligible to a good accuracy.

Using (4) and (5), we now proceed to the construction of an example of a joint eigenstate of commuting periodic functions of Q and P that describes the double-slit setup. For this, the two localized functions $W, \widetilde{M}$ need to be chosen appropriately (Fig. 2). The function W describes the quantum amplitude contained in a single slit. We consider the function that is constant on a single slit (a rectangular shape):

$$W(x) = \chi_{[-a/2,a/2]}(x) = \begin{cases} 1 & \text{for} \quad x \in [-a/2, a/2], \\ 0 & \text{for} \quad x \notin [-a/2, a/2]. \end{cases} \tag{6}$$

Here, a is the width of the slit. This is illustrated in Fig. 2(a). The expression for the Fourier transform of W is

$$\widetilde{W}(k) \propto \operatorname{sinc}(ak/2).$$

The function $\widetilde{W}$ accounts for the modulation of the interference pattern $I(k)$. In the case of a double slit interference experiment with slit separation $T > a$, the known interference pattern $I_{ds}(k)$ is of the form

$$I_{ds}(k) \propto \operatorname{sinc}^2(ak/2)\cos^2(Tk/2).$$

The cosine describes a repeated pattern, and it suggests that we choose $\widetilde{M}$ to correspond to a single instance of this pattern (in practice, this choice would be made based on experimental data):

$$\widetilde{M}(k) = \cos(T'k/2)\,\chi_{[-\pi/T',\pi/T']}(k) = \begin{cases} \cos(T'k/2) & \text{for} \quad k \in [-\pi/T', \pi/T'], \\ 0 & \text{for} \quad k \notin [-\pi/T', \pi/T']. \end{cases} \tag{7}$$

This is illustrated in Fig. 2(b). For the $2\pi/T$-periodic set

$$Y = \bigcup_{n=-\infty}^{\infty} [2\pi n/T - \pi/T', 2\pi n/T + \pi/T']$$

to be different from the whole real line, it is required that $T' > T$, so that the interval $[-\pi/T', \pi/T']$ is strictly contained in the interval $[-\pi/T, \pi/T]$.

Combining the expressions obtained for $\widetilde{W}, \widetilde{M}$ the interference pattern is described by

$$|\widetilde{\psi}_2(k)|^2 \propto \frac{1}{T^2}\operatorname{sinc}^2(ak/2) \sum_{n=-\infty}^{\infty} \cos^2\left[\frac{T'}{2}\left(k + \frac{2\pi n}{T}\right)\right] \times \chi_{[-\pi/T',\pi/T']}\left(k + \frac{2\pi n}{T}\right). \tag{8}$$

This is a sum of non-overlapping terms, and the support of this function is the periodic set Y that is made up of equidistant copies of the interval $[-\pi/T', \pi/T']$. For the quantum state in position space, W is as defined in (6), and M follows from $\widetilde{M}$ as defined in (7):

$$\psi_2(x) \propto \{W * [\Delta_T((\cdot) - T/2)\, M]\}(x) = \sum_{n=-\infty}^{\infty} M((n-1/2)T)\,\chi_{[(n-1/2)T - a/2, (n-1/2)T + a/2]}(x). \tag{9}$$

The Dirac comb is shifted by $T/2$, in correspondence with the experimental setup. (This shift becomes a phase factor in momentum space and does not affect the momentum distribution.) Figures 2(c) and 2(d) illustrate ψ and $\widetilde{\psi}$ as constructed in (9) and (8), respectively.

There are two important limiting cases. The spectral projection $\chi_Y(P)$ is over a strictly periodic set Y. In contrast, the dimensions of any experiment are necessarily finite, and, in particular, the experiment reported in [2] was performed with a total of six wires only, preparing the state $\chi_B(P)\psi$, where B is the complement to the region occupied by the wires. A model calculation shows that the difference between the states $\chi_B(P)\psi$ and $\chi_Y(P)\psi$ is undetectable given the accuracy of the experiment at hand.

Finally we may consider the limiting case where $T' \to T$. This corresponds to the wires becoming negligibly thin. When $T' = T$ the function M is zero at every delta peak of the periodic Dirac comb, except for two locations: $x = -T/2$ and $x = +T/2$. Hence it follows that for this particular choice of $W, \widetilde{M}$, the quantum state ψ_2 exists solely in the two slits and is an approximation to a joint eigenstate defined on periodic sets, where the wires must be assumed to have a very small thickness. The experimental setup considered prepares this quantum state at the aperture at location (i) as an eigenstate of $\chi_X(Q)$ for the periodic set X. Passage through a periodic wire set Y will cause a projection of the state onto one that is

a proper joint eigenstate of periodic position and momentum sets. This projective measurement action causes a disturbance of the incoming 2-slit wave function, which manifests itself in the observed position distribution at (iii): In an ideal setup with dimensions identical to those reported in [2], 1% of the total probability would not be found in the two detectors at (iii) where it would otherwise be expected. Instead, this one percent of probability would be distributed over the remainder of the periodic set X. According to [2], for the double-pinhole setup about 2% probability were found outside of the main peaks.

V. DISCUSSION AND OUTLOOK

A description of multislit experiments was presented, and in particular of the modified double-slit experiment in [2], in terms of quantum states that are defined on periodic intervals of position and momentum. These quantum states, themselves not periodic, represent a class of joint eigenstates of periodic functions of position and momentum. Using a description in terms of such joint eigenstates it was possible to account for the two observations reported in [2] concerning the behavior of a double-slit input state ψ_2 and a single-slit input state ψ_1.

First, an incoming double-slit superposition state is virtually unaffected by the indirect measurement of the interference pattern performed by the wire grating, with each of the wires placed at a node. This is, of course, because the superposition state shows an interference pattern. An explanation in terms of joint eigenstates over periodic sets, though, goes further and makes it possible to explain why a superposition state can be localized on essentially the same set of positions after it was subjected to such a measurement—after all, measuring the interference pattern corresponds to measuring the momentum distribution. The information about position and momentum of the superposition state is approximately represented by commuting observables. It follows that there is no conflict with the principle of complementarity. The experimental setup constitutes a good approximation to a joint determination of compatible coarse grainings of position and momentum.

Second, an incoming single-slit state does not remain unchanged on passage through the wire system, but is instead detected on a set of locations expected of a joint eigenstate of projectors onto periodic sets in position and momentum space. The additional intensity peaks are found, such that each peak is separated by the same distance from its immediate neighbors as the two slits in the aperture. This is compatible with the interpretation that the single-slit state was projected onto an approximate joint eigenstate of spectral projections of position and momentum on periodic sets. Indeed, the original single-slit state, being already localized on a periodic set, has been changed into a state that is a good approximation to a joint eigenstate through the projective action of the wire grating.

The fact that a single-slit input state is affected by the wire grating in such a way that the detected output state is found to be localized in many periodically spaced intervals is a demonstration of the mutual disturbance of measurements of incompatible observables. The projector $\chi_A(Q)$ onto a state localized in the single-slit region A is not compatible with the projector $\chi_B(P)$ onto a state localized in the set B of intervals in momentum space defined by the gaps in the wire grating or its idealized substitution by a periodic set. Consequently, a state originally prepared to be localized in A is changed by the projective action of the wires so as to be less well localized in A and instead localized in a periodic set.

In this way the present experiment serves as a beautiful, new demonstration of complementarity that complements the existing illustrations. Usually one considers a perfect interference setup and then shows how the interference pattern is degraded by the introduction of a path-marking interaction with a probe system storing (partial) path information. Here one starts with a perfect path-marking setup which then, by introducing the wires, is changed into an interference experiment, degrading the accuracy of path determination.

Finally, we used a construction of a specific class of joint eigenstates of periodic sets of position and momentum, which showed that in an idealized experiment with periodically placed slits and wires one can input such states that would propagate entirely unchanged through the setup, so that the presence of the interference pattern would be established without disturbing the quantum state at all. The work of Corcoran and Pasch [7] suggests that the construction of realistic approximations to such quantum states is possible experimentally as well.

It is interesting to note that the work of [4] has been developed further in [8] and [9]. Modular (periodic) momentum variables are introduced there since they are found to be sensitive to relative phase shift of spatially non-overlapping partial wave functions and are thus indicators of the disappearance of interference fringes due to a path measurement. By comparison, here we are concerned with the diminishing path knowledge from creating an interference pattern, for which we found periodic characteristic functions of Q and P particularly useful. The cited work also introduces uncertainty relations allowing a quantitative description of the trade-off between path knowledge and quality of interference. It seems that there is an intimate connection between these uncertainty relations involving modular variables and trade-off relations between the overall width of a wave function and the fine structure of its Fourier transform that were formulated in [10]; an application of the latter uncertainty relation to the present experiment and a comparison with the uncertainty relation for modular variables are work in progress.

To summarize, we have shown that it is appropriate to view the experiment reported in [2] as a preparation procedure for approximate joint eigenstates on periodic sets of position and momentum, whatever the input state. The validity of this interpretation can be supported by numerical simulations of the experiment and variants of it (with different numbers and thickness of the wires) [11].

ACKNOWLEDGMENTS

We wish to thank Stefan Weigert for pointing out Ref. [7] to us and for valuable comments and suggestions on a draft version of this paper. Thanks are also due to Tom Bullock and Leon Loveridge for a critical reading of the manuscript. We are grateful to Pérola Milman and an anonymous referee for pointing out Ref. [4].

APPENDIX A: DETERMINATION OF THE MOMENTUM DISTRIBUTION VIA LATE-TIME POSITION MEASUREMENT

From classical optics it is known that the interference pattern of a wave passing through a double slit can be described by the Fourier-transformed aperture profile. Additional analysis is necessary to justify the same application in quantum mechanics. In particular, it is required to show that after free evolution the position representation of the state ψ_t at location (ii) is, up to scaling, approximated by the momentum representation of ψ_0, at the aperture at (i):

$$\psi_t \propto \widetilde{\psi}_0 \quad \text{(approximately)}.$$

We give a simple "rough and ready" argument here to show how this approximation can be obtained. The solution of the Schrödinger equation for free time evolution is given by

$$\psi_t(x) = \sqrt{\frac{m}{2\pi i t}} \int_{-\infty}^{+\infty} \psi_0(x') \exp\left(i\frac{m(x-x')^2}{2t}\right) dx'.$$

With the limits of integration bounded by the apertures, the actual integration takes place from $-(T+a)/2$ to $(T+a)/2$. In the limit of large t then, the term depending on $(x')^2$ in the exponential can be neglected to a good approximation, because it is bounded by the finite dimensions of the aperture:

$$\psi_t(x) \approx \sqrt{\frac{m}{2\pi i t}} \int \psi_0(x') \exp\left(i\frac{mx^2}{2t}\right) \exp\left(i\frac{mx}{t}x'\right) dx'.$$

After trivial rearranging, the desired expression is obtained:

$$\begin{aligned}\psi_t(x) &\approx \sqrt{\frac{m}{it}}\, e^{i(mx^2/2t)} \frac{1}{\sqrt{2\pi}} \int \psi_0(x')\, e^{i(mx/t)x'} dx' \\ &\approx \sqrt{\frac{m}{it}} \exp\left(i\frac{mx^2}{2t}\right) \widetilde{\psi}_0\left(\frac{m}{t}x\right).\end{aligned}$$

The parameter t can be eliminated using $\frac{p_z}{m}t = L$, with the distance to the lens $L = 0.55m$, where p_z denotes the longitudinal momentum component. In doing so, the limit of large t becomes a limit of large distance L in relation to the aperture size. Considering the dimensions of the setup used in [2], where the center-to-center separation of the two pinholes is 0.25 mm, this is reasonable. Furthermore, as p_x/p_z will be small given these dimensions, we can also substitute p_z approximately with the magnitude of the mean momentum p_0 so that for the mean wavelength λ of the packet we can use the value $\lambda = 2\pi/p_0 \approx 2\pi/p_z$, and so $t \approx mL\lambda/(2\pi)$. This gives the intensity as

$$|\psi_t(x)|^2 \approx \frac{2\pi}{L\lambda} \left|\widetilde{\psi}_0\left(\frac{2\pi}{L\lambda}x\right)\right|^2.$$

Hence, measuring the interference pattern at location (ii) by determining the distribution of position Q constitutes a measurement of a scaled momentum observable with respect to the input state ψ_0. We can express this in terms of the spectral measures of Q and P:

$$\langle\psi_t|\chi_{L\lambda Z/(2\pi)}(Q)\psi_t\rangle \approx \langle\psi_0|\chi_Z(P)\psi_0\rangle,$$

where Z is any (Borel) subset of $\mathbb{R}$. The separation of the wires in Fig. 1 was indicated as being proportional to $2\pi/T$; the above consideration gives the separation in spatial dimensions as $L\lambda/T$.

APPENDIX B: SQUARE INTEGRABILITY

The relation (3) may be used to define a wave function ψ via Eqs. (4) and (5) for square-integrable W, M if W vanishes outside an interval of length strictly less than T, because then the square-integrability condition is met, i.e., if the L^2 norm of $||\psi||_2$ is finite:

$$\begin{aligned}||\psi||_2 &= \int_{-\infty}^{+\infty} |W * (\Delta_T\, M)(x)|^2\, dx = \int \overline{W * \left[\sum_{n=-\infty}^{\infty} \delta((\cdot) - nT)\, M\right](x)}\; W * \left[\sum_{n'=-\infty}^{\infty} \delta((\cdot) - n'T)\, M\right](x)\, dx \\ &= \int \overline{W * \left[\sum_n \delta((\cdot) - nT) M(nT)\right](x)}\; W * \left[\sum_{n'} \delta((\cdot) - n'T) M(n'T)\right](x)\, dx \\ &= \int \sum_n \overline{W(x-nT)}\, \overline{M(nT)} \sum_{n'} W(x-n'T) M(n'T)\, dx = \sum_n |M(nT)|^2 \int |W(x-nT)|^2\, dx = \|W\|_2^2 \sum_n |M(nT)|^2.\end{aligned}$$

The last line is obtained due to the localization property of the function W, which entails that $\overline{W(x-nT)}W(x-n'T) = 0$ if $n \neq n'$. The square integrability of the Fourier transform $\widetilde{\psi}$ is ensured by the Fourier-Plancherel theorem.

APPENDIX C: NO DELTA FUNCTIONS BEYOND THIS POINT

The construction of Sec. IV involved delta functions; here a different approach is presented that is mathematically rigorous without going into the theory of distributions. While similar to [6], the result here is more general.

Starting by choosing a square-integrable function W with support strictly within the interval $(-T/2, T/2)$, we define a periodically supported function ψ as

$$\psi(x) = \sum_{n=-\infty}^{\infty} c_n\, W(x - nT).$$

For each x, the sum contains exactly one term; hence the series converges pointwise. The coefficients c_n are to be determined

by further constraints below; here we note that given the square integrability of W, ψ is square integrable if and only if the c_n are square summable. This entails that the series also converges in norm. Note that

$$\text{supp}\ \psi = \bigcup_{n=-\infty}^{\infty} \text{supp}\,(W + nT)\,.$$

Computing the Fourier transform yields

$$\begin{aligned}\widetilde{\psi}(k) &= \int_{-\infty}^{\infty} \sum_{n=-\infty}^{\infty} c_n\, W(x - nT)\, e^{ikx}\, dx \\ &= \sum_{n=-\infty}^{\infty} c_n\, e^{iknT}\, \widetilde{W}(k). \end{aligned} \tag{C1}$$

The coefficients c_n represent the coefficients of a Fourier series expansion of a periodic function $\widetilde{M}_p$ with period $2\pi/T$:

$$\widetilde{M}_p(k) = \sum_{n=-\infty}^{\infty} c_n\, e^{i\,k\,nT}.$$

Let $\widetilde{M}$ be a function that is supported inside the interval $[-d,d]$ where $0 < d < \pi/T$. We can then specify $\widetilde{M}_p$—and hence the coefficients c_n—so that

$$\widetilde{M}_p(k) = \sum_{n=-\infty}^{\infty} \widetilde{M}\left(k - \frac{2\pi}{T}n\right).$$

This function is supported in a periodic set,

$$\text{supp}\ \widetilde{M}_p \subseteq \bigcup_{n=-\infty}^{\infty} \left[\frac{2\pi}{T}n - d, \frac{2\pi}{T}n + d\right].$$

We thus have that

$$\widetilde{\psi}(k) = \widetilde{M}_p(k)\ \widetilde{W}(k).$$

A simple calculation shows that $\widetilde{M}$ is square integrable if and only if the c_n are square summable. As noted above, this condition is equivalent to ψ being square integrable. With such a choice of $\widetilde{M}$ we can also see directly from the last formula that $\widetilde{\psi}$ is square integrable, in line with the Fourier-Plancherel theorem.

[1] S. Kocsis, B. Braverman, S. Ravets, M. J. Stevens, R. P. Mirin, L. K. Shalm, and A. M. Steinberg, Science **332**, 1170 (2011).

[2] S. S. Afshar, E. Flores, K. F. McDonald, and E. Knoesel, Found. Phys. **37**, 295 (2007).

[3] P. Busch, M. Grabowski, and P. J. Lahti, *Operational Quantum Physics*, Lecture Notes in Physics, Vol. 31 (Springer, 1995) (2nd corr. print 1997).

[4] Y. Aharonov, H. Pendleton, and A. Peterson, Int. J. Theor. Phys. **2**, 213 (1969).

[5] P. Busch and P. J. Lahti, Phys. Lett. A **115**, 259 (1986).

[6] H. Reiter and W. Thirring, Found. Phys. **19**, 1037 (1989).

[7] C. J. Corcoran and K. A. Pasch, J. Phys. A **37**, L461 (2004).

[8] Y. Aharonov and D. Rohrlich, *Quantum Paradoxes: Quantum Theory for the Perplexed*, 1st ed. (Wiley-VCH & Co. KGaA, Weinheim, 2005).

[9] J. Tollaksen, Y. Aharonov, A. Casher, T. Kaufherr, and S. Nussinov, New J. Phys. **12**, 013023 (2010).

[10] J. B. M. Uffink and J. Hilgevoord, Found. Phys. **15**, 925 (1985).

[11] J. C. G. Biniok (unpublished).